The International Journal of Advanced Manufacturing Technology (2024) 134:1463–1485
https://doi.org/10.1007/s00170-024-14126-1

ORIGINAL ARTICLE

# Comparison of reinforcement fibers in 3D printing mortars using multi-criteria analysis

Sara Alonso-Cañon[1] · Elena Blanco-Fernandez[1] · Daniel Castro-Fresno[1] · Adrian I. Yoris-Nobile[1] · Laura Castanon-Jano[1]

Received: 12 September 2023 / Accepted: 9 July 2024 / Published online: 5 August 2024


## Abstract

3D concrete printing (3DCP) has developed rapidly in recent years, with a relatively high amount of mortars emerging apt for 3D printing. Some of these mortars include fibers to improve their strength. Despite mechanical properties having been quite well studied, there still is missing information on cost, printability, and environmental impacts. The objective of this research is to select the best mortars with fibers considering four criteria: printability, mechanical strength, and economic and environmental impact applying a multi-criteria decision-making analysis (MCDMA). Seven types of fibers with different dosages were assessed in the reinforced mortars: zylon, aramid, carbon, glass, cellulose, textile, and polypropylene. AHP method and equal weights were used as ponderation techniques of the criteria while WASPAS and TOPSIS methods were used to calculate the rankings of the MCDMA. Printability was measured through rheological tests using a rotational rheometer, mechanical strength through flexural tests at 28 days based on EN 196–1, and cost just considering the materials and environmental impact through a life cycle assessment (LCA). The results showed that 13-mm-long glass fibers with a content of 0.1% were the best alternative, closely followed by the mortar with 6 mm cellulose fibers with a content of 0.05%. For the best option (G13;0.1), the increments in the printability index, flexural strength, cost, and LCA were − 14.37%, 16.70%, 5.88%, and 2.86%, respectively. It can also be concluded that high elastic modulus fibers (zylon and aramid), although able to increase significantly the flexural strength (up to 30% in the case of zylon), prevent them from being an optimal solution due to their high cost.

**Keywords** 3D concrete printing · Additive manufacturing · Fibers · Multi-criteria decision-making · Mechanical properties · Rheology · Life cycle assessment

## 1 Introduction

Engineering and construction are in continuous development seeking to improve their productivity, incorporating new technologies and techniques. In recent years, the process of additive manufacturing (AM) or 3D concrete printing (3DCP) has had a strong development. This construction system has some advantages over traditional construction, such as the production of complex shapes, the automation of the process, the reduction of waste materials, and the reduction of construction times.

The incorporation of fibers, which are already used in traditional construction, has begun to be tested in the field of concrete 3D printing by some authors using steel [1, 2], carbon [3, 4], glass [5, 6], PVA [7, 8], or polypropylene [9, 10], fibers with the aim of improving the mechanical properties (flexural strength, toughness, impact resistance,

✉ Elena Blanco-Fernandez
elena.blanco@unican.es

Sara Alonso-Cañon
alonso1alonso@gmail.com

Daniel Castro-Fresno
castrod@unican.es

Adrian I. Yoris-Nobile
adrianyoris84@gmail.com

Laura Castanon-Jano
laura.castanon@unican.es

[1] GITECO Research Group, Universidad de Cantabria, Avenida de los Castros 44, 39005 Santander, Spain

plastic shrinkage cracking, etc.), and/or rheological behavior (dynamic viscosity, shear stress, etc.). However, there are no studies using recycled fibers (textile, cellulose) or ultra-high tensile modules (aramid, zylon). In the particular case of cellulose, some authors have already studied their potential application in precast concrete, because of its low cost and environmental impact, adequate mechanical performance, and sufficient durability even when exposed to weathering conditions such as sewage water [11] or carbonation and freeze–thaw cycles [12]; however, there are not yet studies on 3DCP.

Mechanical strength has been largely studied in fiber-reinforced 3DCP by several authors, as reported by Alonso-Cañon in a review paper [13]. The conclusion of this study revealed that adding fibers can increase up to 30% of the flexural strength of 3DCP with respect to a 3DCP without fibers while there are no clear conclusions regarding advantages or disadvantages in compressive strength.

In relation to cost, several studies have attempted to estimate and compare costs associated with reinforced 3D concrete printing (3DCP). The scarcity of cost information and inconsistencies in reporting make it challenging to draw definitive conclusions. Noteworthy findings include Inozemtcev and Duong's comparison, suggesting potential savings of 30–50% in building costs with 3DCP due to reduced material and machinery hours [14]. Kreiger et al. compared various construction technologies, but their estimate of concrete costs at \$144 USD/$m^3$ lacked detailed calculations [15]. García de Soto et al. demonstrated advantages for 3DCP in building non-standard shapes, with costs varying between straight and curved layouts [16]. Nerella et al. reported a 70% higher cost for 3DCP compared to conventional methods using high-performance concrete [17]. Otto et al. assumed a 30% higher cost for 3DCP without explicit calculations [18]. In Han et al.'s study, the environmental and cost analysis undertaken indicated higher costs for 3DCP in building a silo compared to conventional concrete [19]. Abdalla et al. carried out an environmental and economical analysis of a house using conventional methods vs 3DCP; however, concrete cost per $m^3$ data was not shown, hindering a direct comparison between conventional and 3DCP methods [20]. Weng et al. assumed a consistent concrete price for both methods in an environmental and productivity assessment of a concrete bathroom unit [21], despite 3DCP generally having a larger amount of cement, disregarding also differences in compressive strength. Yoris-Nobile et al. compared different mortars for 3D printing, providing cost per ton of material, with costs ranging from 44.80 to 184.18 €/T, depending on the type of mortar used; however, none of the mortars included fibers in the mix [22].

Environmental performance has been considered a key advantage for concrete 3D printing technologies by many authors, basically based on the topological optimization of the shapes and the elimination of formworks. In [23], a multi-criteria decision-making analysis (MCDMA) applying the MIVES and Delphy techniques is proposed and applied to the first 3DCP bridge in the world built in 2016 by Acciona to assess its sustainability performance. The material used was a concrete with 500 kg cement/$m^3$ concrete that incorporated steel fibers and used D-Shape 3D printing technology, and also has post-tensed cables. In this study, greenhouse emissions, energy consumption, and material consumption were considered part of environmental indicators assigning weights to each of them (among other factors) with the Delphy technique. However, greenhouse emissions and energy consumption are somehow correlated. Besides, it is more adequate to consider the global warming potential to deal with greenhouse gas emissions. In [19], an environmental and economic assessment on 3D-printed buildings was carried out. The aim was to compare 3 types of 3DCP vs the other 3 types of concrete for mold casting. In the 3DCP, around 440–455 kg of cement per $m^3$ of concrete was added, while in the mold casting, they added between 320 and 345 kg/$m^3$. In this study, fibers were not added to the concrete. Furthermore, mechanical strength was not considered either, despite the differences in cement content between the C3DP and standard concrete. Instead, it was assumed that both had 30 MPa of nominal compressive strength at 28 days (C30). Thus, environmental comparison of structural concretes without considering their strength is not fully adequate, since the rationale "the more the strength, the least amount of concrete required, the least the cost, the less the environmental impact" should be assumed. In the study of Alhumayani et al. [24], a comparison of 4 alternatives (3DCP, cob-printing, concrete pour casting, cob blocks) of building a structural wall was carried out, without using fibers in any case. The wall thickness and amount of material used of each alternative changed; nevertheless, no data about the bearing capacity of the wall was provided. Therefore, the conclusions regarding the LCA are not fully comparable, since each alternative could have a different bearing capacity. In [25], similarly to [24] also performed a comparison of a bearing wall using 4 alternatives (1 with standard concrete, 3 with 3DCP with or without rebars and different mixes), using fibers in some of the concrete mixes. Again, wall-bearing capacity was not provided; therefore, LCA results are not fully comparable.

The rheological properties play a crucial role in the constructability and printability of cement mortars. To assess these properties, various authors have conducted tests using rotational rheometers, enabling the determination of both yield stress and viscosity values. Jayathilakage conducted a comparative analysis of different rheometers, confirming that torque rheometers yield accurate rheological property values [26]. In another study, Chen introduced retarder dosages into mortar mixtures and observed a decrease in yield

stress values as the dosage increased, resulting in yield stress values ranging from 450 to 750 Pa [27]. Additionally, Kolawole and Banfill investigated the impact of superplasticizer incorporation, revealing a significant reduction in yield stress values (ranging from 550 to 750 Pa), notably lower than the 1100 Pa observed in the control mixture [28, 29]. Conversely, Chen, in his research involving the addition of bentonite to mixtures, found that an increase in bentonite content led to an elevation in yield stress values [30]. Finally, Russel, in a rheological analysis focused on printable concretes, emphasized the critical need to minimize initial yield stress values for these materials [31].

Overall, comparative analyses that consider not only mechanical properties of mortars including fibers, but also their suitability to be printed with a real 3D printer, cost, and environmental impact at the same time, have not yet been carried out so far. This comparison is fundamental because it would provide practical conclusions for 3DCP users who aim to include fibers in their mixes, and that need to take a decision regarding the most adequate type of fiber in order to avoid excessive costs, undesired environmental impact, or printability problems, and what is more, just decide not to use fibers, not to mention new fibers such as aramid, zylon, cellulose, and recycle textile.

## 2 Methodology

### 2.1 Overall procedure

The objective of this paper, based on the gaps found in the state of the art as previously stated, is to determine the best reinforcement fibers and dosages in 3D-printed mortars through a multi-criteria decision-making analysis (MCDMA). These mixtures will be a total of 36 (35 with fibers plus a control mortar without them), in which different types of fibers and percentages of fibers will be combined. Four criteria were selected for the MCDMA: printability, mechanical strength, material cost, and environmental impact, for which different laboratory tests were carried out and a life cycle assessment (LCA) was performed. The Analytic Hierarchy Process (AHP) method and equal weights were used to assign the criteria weights, and the Technique for Order of Preference by Similarity to Ideal Solution (TOPSIS) and Weighted Aggregated Sum Product Assessment (WASPAS) methods were used to assess the MCMDA scores and, thus, rankings. Figure 1 represents the graphical abstract of the whole process carried out.

Firstly, for this purpose, the rheological and mechanical characteristics of the mortars will be analyzed in the laboratory. Secondly, a multi-criteria decision-making analysis will be performed, employing firstly two weighing scenarios (AHP method and equal weights) and two ranking methods (WASPAS and TOPSIS).

Aramid, carbon, glass, cellulose, textile, polypropylene, and zylon fibers were used. In the laboratory, the fiber content that helped to maintain good printability was determined for each type of fiber. Steel fibers were discarded since preliminary tests show that they could get clogged in the screw and, as a result, damage the 3D printer. As the number of fibers increases, workability is lost until the filament starts to get choppy or plugs are produced in the extrusion nozzle. Therefore, the percentages used vary between 0.05 and 0.3. Then, the laboratory tests of flexural strength, compression, and rheology were carried out. In the second part of the study, an MCDMA analysis was proposed, for which two methods were used: WASPAS and TOPSIS. The AHP method and equal weights were used to calculate the

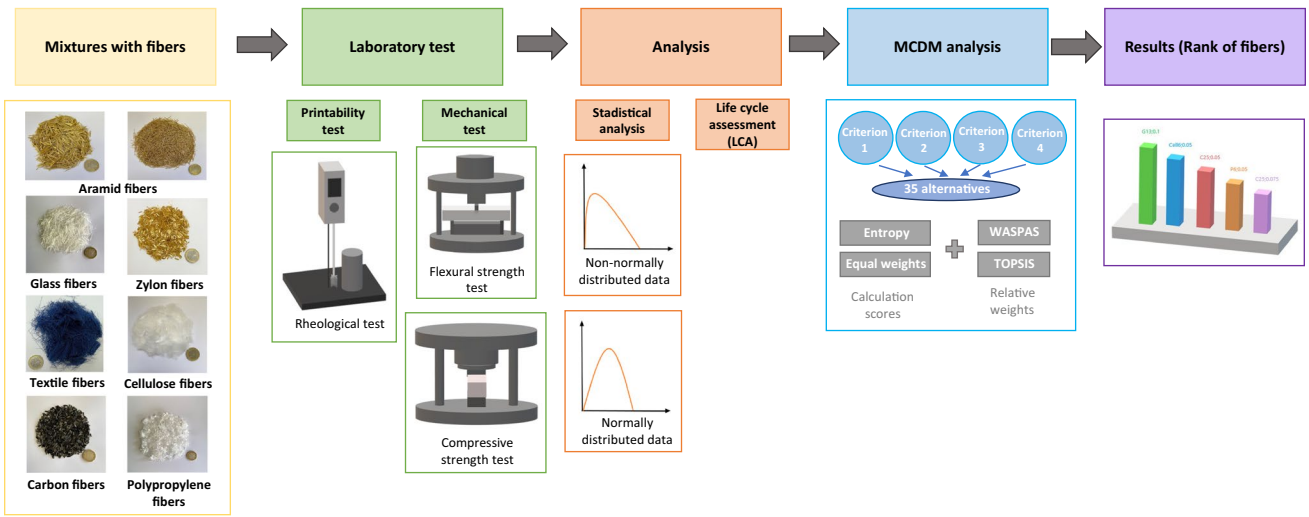


**Fig. 1** Graphical description of the work methodology

relative weights of the criteria. This made it possible to rank and obtain the best fibers for 3D printing. Figure 1 shows a graphical description of the methodology carried out.

## 2.2 Materials and dosages

This study aims to compare and obtain the best 3D printing dosages reinforced with fibers, based on 4 different criteria, such as resistance, cost, environmental impact and printability. Therefore, a total of 54 samples were prepared. A Cement type III/B 32.5 N-SR, which has a clinker content of 31% and 66% blast furnace slag was used. As a fine aggregate, sands of natural origin were used. As a fine material, fly ash was used, with a degree of crystallinity of 35% and a loss on ignition of 3.4%. To add cohesion to the mixture, a small percentage of kaolin was added as an addition. A workability modifier has also been used to give the mixtures the optimum consistency for printing. The selected superplasticizer was Mastersure 950 from BASF.

Finally, seven different types of fibers have been incorporated into the mixtures, whose properties are shown in Table 1. These fibers are aramid, carbon, cellulose, polypropylene, textile, glass, and zylon. Some of these fibers have been supplied in different lengths, varying from 3 to 30 mm.

In terms of the percentages of fibers that have been incorporated, in conventional concrete are below 1%, because a high percentage of fibers significantly reduces the workability of the mixtures [32, 33]. The 3D printing concrete should also maintain low percentages of fibers, so that the mixture can maintain its workability and no plugs are produced in the extrusion nozzle. In this study, the fibers were incorporated in different percentages (0.05; 0.075; 0.1; 0.2; and 0.3) depending on the printability of the mixtures. These percentages vary due to the fact that some of the mixtures with higher ratios begin to cut or to remain blocked in the extrusion nozzle. With the above-mentioned types of fiber and their different percentages, the 35 alternatives that were later used for the multi-criteria analysis were proposed. The fibers used in the study are shown in Fig. 2.

For the study, a reference mixture was used, composed of the aforementioned materials, cement, fly ash, limestone aggregate, kaolin, and superplasticizer, in which the different types of fibers were incorporated in different proportions.

Table 2 shows the dosages of the mixtures according to the percentage of fibers. All dosages are ratios of the cement weight, except the fiber content, which is reported in a fraction of the mixture.

## 2.3 Mixture preparation

A planetary mixer with a capacity of 30 l was used to prepare the mixtures. It has three rotation speeds: 142 (slow), 234 (medium), and 429 rpm (fast), but in our production, we only used the first two. First, the dry materials, cement, fly ash, kaolin, and aggregates, were mixed for 15 s at slow speed. Then, the water was gradually added and mixed for 2 min with the dry materials. Subsequently, to achieve the right consistency, the plasticizer was added and mixed for one and a half minutes. Later, the fibers were added gradually, to obtain a good dispersion and mixed for half a minute. Finally, to complete the mixing process, the mixer speed was changed to medium and it started to mix for two more minutes.

For the testing of the study, a Delta-type printer has been used, model "WASP 3MT," which is based on EMS technology and that helps to develop the elements by extrusion. This model has two different parts: the control panel and the printing system. The control panel allows to adjust the

**Table 1** Physical properties and composition of the fibers

| | Type | Color | Length (mm) | Diameter (μm) | Density (g/cm$^3$) | Tensile strength (MPa) | Elastic modulus (GPa) | Elongation (%) |
|---|---|---|---|---|---|---|---|---|
| Aramid | Non-bundled short cut | Gold | 6 | 21 | 1.39 | 3200 | 73 | 4.3 |
| | Non-bundled short cut | Gold | 12 | 21 | 1.39 | 3200 | 73 | 4.3 |
| | Bundled dipped chopped | Gold | 20 | 420 | 1.35 | 2600 | 68 | 4.3 |
| | Bundled dipped chopped | Gold | 30 | 420 | 1.35 | 2600 | 68 | 4.3 |
| Carbon | Chopped | Black | 6 | 7 | 1.8 | 4280 | 232 | 1.8 |
| | Chopped | Black | 25 | 7 | 1.78 | 4300 | 234 | 1.8 |
| Cellulose | Round monofilament | White | 6 | 18–48 | 0.91 | 460 | 3.85 | 15 |
| | Round monofilament | White | 20 | 18–48 | 0.91 | 460 | 3.85 | 15 |
| Glass | Multi-filament | White | 13.1 | 13.5 | 2.68 | 1620 | 74 | |
| Zylon | Multi-filament chopped | Gold | 6 | | 1.56 | 5800 | 270 | 2.5 |
| Textile | | Blue | 20 | 150–170 | 1.24 | | | |
| Polypropylene | Monofilament | White | 6 | 31 | 0.91 | | 1.5 | |


**Fig. 2** Fibers used: **a** aramid fibers non-bundled short cut. **b** Aramid fibers bundled dipped chopped. **c** Glass fibers. **d** Zylon fibers. **e** Polypropylene fibers. **f** Carbon fibers. **g** Textile fibers. **h** Cellulose fibers

**Table 2** Mixture proportions

| Mixtures | Cement | Limestone aggregate | Water | Superplasticizer | Fly ash | Kaolin | Fibers (%) |
|---|---|---|---|---|---|---|---|
| F0.05 | 1 | 2 | 0.5338 | 0.0093 | 0.5 | 0.0417 | 0.05% |
| F0.075 | 1 | 2 | 0.5338 | 0.0093 | 0.5 | 0.0417 | 0.075% |
| F0.1 | 1 | 2 | 0.5338 | 0.0093 | 0.5 | 0.0417 | 0.1% |
| F0.2 | 1 | 2 | 0.5338 | 0.0093 | 0.5 | 0.0417 | 0.2% |
| F0.3 | 1 | 2 | 0.5338 | 0.0093 | 0.5 | 0.0417 | 0.3% |

different variables, such as the printing speed, height, and coordinates where the nozzle starts printing and the diameter of the layers. The printing system, in turn, is composed of three articulated arms disposed in a triangular configuration corresponding to the x, y, and z axes. It also has a hopper, inside which is an endless screw, connected to an electric motor, which allows the material to move to the nozzle while it is turning. The nozzle, which was modified and made of TPU, has a circular section of 20 mm in diameter.

## 2.4 Laboratory tests

For the preparation of this study, the mechanical and rheological characterization of the mixtures was carried out.

#### 2.4.1 Preliminary printing trials

3D printing by extrusion requires specific rheological properties of the mixtures in the fresh state. These must have good workability and flowability, allowing the material to be extruded through the screw and nozzle of the 3D printer placing a continuous filament. But once the layers have been extruded, they must have sufficient self-supporting capacity to maintain their shape and support the weight of the upper layers. Thus, preliminary printing trials were performed in order to realize visual analyses of how certain mortars could be more or less suitable for printing purposes (Fig. 3). The printing parameters used for carrying out the preliminary tests of the mortars were the same: 20 mm nozzle diameter (16 mm software input to force overlap), 8 mm layer height, 70 mm/s maximum head speed, 300 rpm screw speed. As it can be seen in Fig. 3, two parallel filaments were printed to form the vertical walls.

#### 2.4.2 Rheological tests

A correlation between printability (based on visual observations during the printing trials) and the parameter yield stress*viscosity is proposed, the so-called printability index. Therefore, good printability (which means a combination of continuity of the extruded filament and self-bearing capacity of the filaments) is correlated, somehow, with a low value of the printability index.

For rheological characterization, a torque rheometer was used. It consists of three parts: an agitator, a cylindrical container, and a cross-shaped paddle. The agitator, with a range of rotation speeds between 10 and 2000 rpm, is connected to a computer to collect the torque values corresponding to the different speeds. A cross-shaped paddle with a height of 5 cm and a radius of 2.5 cm will be placed on the vertical axis of the agitator. Lastly, a cylindrical steel container with an inner diameter of 8 mm and outer diameter of 8.8 cm was adjusted to the characteristics of the materials used [34–37].

**Fig. 3** Preliminary printing trials

The rheological behavior of fresh concrete is considered to correspond to the Bingham model, governed by the following equation:$\tau = \tau_o + \eta\dot{\gamma}$, where $\tau_o$ is the yield stress and $\eta$ refers to the dynamic viscosity of the mixture. In order to perform the test, speeds, which are gradually decreasing, are set, while the torque data obtained are recorded. With these data, the following equations are applied to obtain the shear rate-shear stress parameters [38, 39].

To obtain the shear rate, $\dot{\gamma}$:

$$\dot{\gamma} = 2M\frac{d\Omega}{dM},\ if\ \tau_c \le \tau_o \le \tau_b \tag{1}$$

$$\dot{\gamma} = 2\frac{M\frac{d\Omega}{dM}}{\left(1-\frac{R_b^2}{R_c^2}\right)} - \frac{\Omega - M\frac{d\Omega}{dM}}{\ln\left(\frac{R_b}{R_c}\right)},\ if\ \tau_c > \tau_o \tag{2}$$

$$\dot{\gamma} = max(equation(1); equation(2)) \tag{3}$$

$$\frac{d\Omega}{dM} = \frac{\Omega_j - \Omega_{j-1}}{M_j - M_{j-1}} \tag{4}$$

where $M$ is the torque, $\Omega$ is the rotational speed, $\tau_b$ and $\tau_c$ are the shear stresses on the inner and outer cylinders, Rc is the radius of the cylinders, and Rb and h are respectively the radious and height of the blade.

To calculate the shear stress, τ:

$$\tau_b = \frac{M}{2hR_b^2} \tag{5}$$

$$\tau = \frac{1}{2}\left(\tau_j + \tau_{j+1}\right) \tag{6}$$

With the obtained parameters of shear stress and shear rate, a curve is plotted, which gives the values of yield stress and viscosity.

#### 2.4.3 Mechanical tests

For the mechanical characterization, flexural and compression tests were carried out, using prismatic specimens of 40 mm × 40 mm × 160 mm following the EN 196–1 standard (Fig. 4).

Toughness was not studied, although the influence that fibers have in making concrete tougher (more energy at failure with respect to concrete without fibers) is well known, since it is believed that there will be somehow a correlation between toughness and flexural strength. Another reason of not measuring toughness is that there is no clear consensus on how to measure the area under the stress–strain curve, either in a tensile test or in a flexural test. In [40], toughness is measured through the so-called performance level which represents the energy absorbed up to the peak load in a tensile test. In [41], toughness is measured in a flexural test until a deformation that represents 1/150 of the span. In [42], a withdrawn standard with no replacement, toughness is measured through the "toughness index," which is a relative measure of an area defined for different values of deformation. Therefore, depending on how toughness is measured, results could change. For the purpose of carrying out an MCDMA, it was considered more simple and robust to take only the flexural resistance of prismatic samples according to EN 196–1 [43].

It was also considered relevant to measure the compression strength of fiber-reinforced mortars because some authors have pointed out that the use of fibers might have a negative influence on their compressive strength while others state that it could be the same or even improve [44, 45]. Since there is no general consensus, it was considered relevant to measure it in this research.

Even though some studies pointed out that the printing process might affect the anisotropy [46], not all authors agree with the degree of influence of these input variables in the final strength, since it depends on the printing path, the ratio between nozzle size and fiber length, the rheological properties of the fresh mortar, and the setting time of mortar, among others. Since it is quite common in 3D printing practice that the path pattern alternates printing directions layer by layer, anisotropy loses its influence somehow. This effect of bonding filaments in the same 3D printing plane takes more importance especially when using more fluid mixes, where the extruded filaments can bond one to another without leaving large gaps between them which is the main responsibility of anisotropy. Furthermore, if mortar has a sufficient setting time window, bonding between layers can occur without generating anisotropy between the printing plane and its perpendicular direction, or even between 3D-printed samples and cast samples [47]. The further anisotropy that fibers might introduce in the 3D-printed mortar also depends mainly on the ratio between nozzle size and fiber length, being the nozzle diameter dependent on each particular 3D printer used.

Therefore, in order to simplify the mechanical tests, prismatic samples were fabricated with cast mortar. It is assumed then that even though the mechanical properties of 3D-printed samples might vary a little bit with respect to cast samples, the relative differences between dosages would not be substantially altered. To calculate the flexural strength, the three-point loading method is used, with a loading rate of 50 N/s until failure, following the EN 196–1 standard. Once the maximum force $F_f$ is measured, the flexural strength is calculated with the following equation:

$$f_s = \frac{1.5F_f l}{b^3} \tag{7}$$

where $F_f$ is the flexural strength (MPa), $l$ is the distance between supports (mm), and $b$ is the side of the square section of the prism (mm).

To perform the compression test, the half-prisms broken in the flexural strength test are used. A load is applied uniformly at a loading rate of 2400 N/s, during the whole time of application of the load until the breakage. Once the maximum load to failure is obtained Fc, the compressive strength is calculated with the following equation:

$$C_s = \frac{F_c}{b^2} \tag{8}$$

**Fig. 4** Prismatic samples after flexural test (left) and compression test (right). Mortar with PP fibers

### 2.5 Life cycle assessment (LCA)

An environmental analysis of the different mixtures developed was carried out, using the LCA methodology, based on ISO 14040:2006 [48] and 14044:2006 [49]. A gate-to-gate approach was selected by taking only into account the material production stage. The reference unit was 1 t of mortar. Calculations were performed using the SimaPro software.

Inventory values for the electricity of the mixture and 3D printer, cement, limestone aggregate, superplasticizer, kaolin, and water were collected from the Ecoinvent v3.10 cut-off database [50] as listed in Table 3. Concerning fly ash, as it is considered a waste material resulting from the electricity production in coal power plants, no environmental burdens have been considered [51]. However, for their use in mortar dosages, they need milling and grinding, drying, and transport processes, which involve energy consumption. As there is no data available on the consumption of these processes, an impact factor of 0.027 kg CO2-e/kg proposed by Turner [52] was applied. As for carbon, glass, cellulose, textiles, and polypropylene fibers were also found in the Ecoinvent database. On the other hand, aramid and zylon fibers were not found in that database. The aramid was extracted from the GaBi V9.1 database, while in the case of zylon fibers, Cao et al. [53] presented in their study the components of the material. Finally, the electricity consumption during the mixing and printing processes was measured at the laboratory, resulting in 9.4 kWh and 18.5 kWh.

The EF 3.0 method was selected to transform the resources and the emissions obtained during the inventory phase into impacts. This method has been developed by the European Commission, to establish a common European methodology for the development of LCA. The categories of impacts and their units are shown in Table 4.

The normalization factors used in this work are those included in the Environmental Footprint (EF) method that are based on the study by [54], where global emissions and resource uses were collected and characterized. For the calculation of the normalization factors (NFs), the characterization factors used in the International Reference Life Cycle Data System (ILCD) and the EF methods were applied.

As for the weighting factors, the Joint Research Center (JRC) recommended a set of weighting factors for the European Footprint method [55]. For the development of these weighting set, two different methods were adopted by JRC. The first one consisted in a panel-based approach, involving two target groups: general population and experts in the LCA field. The second method involved a hybrid evidence-based and expert-judgement approach. A final weighting set was recommended by the combination of the results from both methods and incorporating robustness factors.

**Table 3** Datasets

| Material/process | Dataset | Source |
|---|---|---|
| Cement | Cement, blast furnace slag, 66–80% {Europe without Switzerland}\| cement production, blast furnace slag 66–80% \| Cut-off, U | Ecoinvent v3.10 |
| Limestone aggregate | Limestone, crushed, washed {RoW}\| market for limestone, crushed, washed \| Cut-off, U | Ecoinvent v3.10 |
| Water | Tap water {Europe without Switzerland}\| tap water production, conventional treatment \| Cut-off, U | Ecoinvent v3.10 |
| SP | Plasticiser, for concrete, based on sulfonated melamine formaldehyde {GLO}\| market for \| Cut-off, U | Ecoinvent v3.10 |
| Kaolin | Kaolin {GLO}\| market for \| Cut-off, U | Ecoinvent v3.10 |
| Carbon fibers | Acrylonitrile–butadiene–styrene copolymer {GLO}\| market for \| Cut-off, U | Ecoinvent v3.10 |
| Cellulose fibers | cellulose fiber {RoW}\| market for cellulose fiber \| Cut-off, U | Ecoinvent v3.10 |
| Glass fibers | Glass fiber {GLO}\| market for \| Cut-off, U | Ecoinvent v3.10 |
| Polypropilene fibers | Polypropylene, granulate {GLO}\| market for \| Cut-off, U | Ecoinvent v3.10 |
| Textile fibers | Fiber, cotton {GLO}\| market for fiber, cotton \| Cut-off, U | Ecoinvent v3.10 |
| Aramid fibers | Aramid fiber (para aramid). Condensation of para- phenylene diamine and terephthaloyl dichloride; single route, at plant; para aramid (en) | GaBi V9.1 |
| Zylon fibers | Purified terephthalic acid {RoW}\| production \| Cut-off, U | Cao et al. [53] |
| | Phosphoric acid, fertiliser grade, without water, in 70% solution state {RoW}\| phosphoric acid production, dihydrate process \| Cut-off, U | |
| | Inorganic phosphorus fertiliser, as P2O5 {RoW}\| market for inorganic phosphorus fertiliser, as P2O5 \| Cut-off, U | |
| | Benzimidazole-compound {RoW}\| production \| Cut-off, U | |
| Electricity mixer and 3D printer | Electricity, low voltage {ES}\| market for \| Cut-off, U | Ecoinvent v3.10 |

**Table 4** Environmental categories, units, normalization, and weighting factors (EF 3.0 method)

| Environmental categories | Un | Normalization | Weighting |
|---|---|---|---|
| Climate change | kg CO2 eq | 0.0001235 | 21.06 |
| Ozone depletion | kg CFC11 eq | 18.64 | 6.31 |
| Ionizing radiation | kBq U-235 eq | 0.000237 | 5.01 |
| Photochemical ozone formation | kg NMVOC eq | 0.02463 | 4.78 |
| Particulate matter | disease inc | 1680 | 8.96 |
| Human toxicity, non-cancer | CTUh | 4354 | 1.84 |
| Human toxicity, cancer | CTUh | 59,173 | 2.13 |
| Acidification | mol H + eq | 0.018 | 6.2 |
| Eutrophication, freshwater | kg P eq | 0.6223 | 2.8 |
| Eutrophication, marine | kg N eq | 0.05116 | 2.96 |
| Eutrophication, terrestrial | mol N eq | 0.005658 | 3.71 |
| Ecotoxicity, freshwater | CTUe | 0.00002343 | 1.92 |
| Land use | Pt | 0.00000122 | 7.94 |
| Water use | m3 depriv | 0.00008719 | 8.51 |
| Resource use, fossils | MJ | 0.00001538 | 8.32 |
| Resource use, minerals, and metals | kg Sb eq | 15.71 | 7.55 |

However, the results of the LCA must be fed into the multi-criteria analysis, so we need to transform these category indicator results into a single value of environmental impact for each dosage analyzed. For this, two more steps are carried out: normalization and weighting. Normalization helps to convert the results of the environmental categories into neutral global units, to determine the relative importance of the results by dividing by a reference value. Meanwhile, weighting converts, by means of numerical factors, the normalized values so that they can be added together to obtain a single result. The normalization and weighting values used are those proposed in the EF 3.0 method and are shown in Table 4.

## 2.6 Cost

Another criterion established for the MCDM analysis was the total cost of each mixture (in euro/ton). This was computed for each alternative by summation of individual cost of cement, aggregates, fly ash, kaolin, superplasticizer, and fibers. The individual costs of each of the materials that make up the different mixes are shown in Table 5. The costs of each of the fibers were provided by the different suppliers, with the exception of the textile fibers, which are considered free of cost since they are a waste from the textile industry, which would be put to a new use.

## 2.7 Multi-criteria decision-making analysis (MCDMA)

The selection of the optimal fibers and percentages to incorporate into 3D printing mixtures involves several factors, that can be contradictory in many cases, such as printability and strength. The MCMD allows rational decisions to be made on the basis of the different criteria that are important for the choice of fibers. In this study, we use two different methods, WASPAS and TOPSIS, to obtain the ranking of alternatives. For assigning weighs, two methods were considered: AHP and equal weighs.

The four criteria considered were (1) printability, (2) mechanical resistance, (3) economic, and (4) environmental impact. The indicators that have been used to assess those criteria were, respectively, (1) yield stress*dynamic viscosity (Pa^2*s), (2) flexural strength (MPa), (3) cost of materials (€/T), and (4) points of an LCA.

### 2.7.1 WASPAS method

The first method to be used for decision-making will be the Weighted Aggregated Sum Product Assessment (WASPAS). This has been developed by Zavadskas et al. [56] and

**Table 5** Cost of individual materials

| Mortar | Cement | Fly ash | Kaolin | | Aggregate | Superplasticizer | |
|---|---|---|---|---|---|---|---|
| Cost (€/kg) | 0.11 | 0.08 | 0.15 | | 0.01 | 2.63 | |
| Fibers | Aramid | Carbon | Cellulose | Glass | Zylon | Textile | Polypropylene |
| Cost (€/kg) | 39 | 26 | 1.35 | 5.8 | 200 | - | 23.2 |

is a combination of other two MCDMs known, namely the Weighted Product Model (WPM) and the Weighted Sum Model (WSM). By combining the two models, it has become a very robust method [57], which has been employed in numerous engineering fields. The steps of the WASPAS method are described below:

Step 1: Definition of the decision-making problem and obtaining the decision matrix. The matrix has the following form:

$X = \left[x_{ij}\right] = m \times n$ , where $m$ represents the defined alternatives, and $n$ the selected criteria.

Step 2: Normalization of the decision matrix. For these, the comparative importance of the criteria is defined, identifying beneficial and non-beneficial criteria, using the following equations:

$$Beneficial\ criteria: \bar{x}_{ij} = \frac{(x_{ij})}{max_i(x_{ij})} \tag{9}$$

$$Non\ beneficial\ criteria: \bar{x}_{ij} = \frac{min_i(x_{ij})}{(x_{ij})} \tag{10}$$

Step 3: Determine the total relative importance of each alternative. For this purpose, the Weighted Sum Model (WSM) is used, defined by the following equation:

$$Q_i^1 = \sum_{j=1}^{n} w_j \cdot \bar{x}_{ij} \tag{11}$$

where $w_j$ is the weight of each criteria, which is obtained with the weighing method (in our case AHP method or equal weights).

Step 4: Determine the total relative importance of each alternative, using now the Weighted Product Model (WPM):

$$Q_i^2 = \prod_{j=1}^{n} \left(\bar{x}_{ij}\right)^{w_j} \tag{12}$$

Step 5: Apply a joint criterion. For this purpose, both methods are combined by means of the following equation:

$$Q_i = \lambda Q_i^1 + (1 - \lambda) Q_i^2 \tag{13}$$

where $\lambda$ is a coefficient that linearly combines both models. The value that is usually used and that will be used in this study is 0.5, since it gives the same weight to both models, although this can be varied.

#### 2.7.2 TOPSIS method

The TOPSIS method, developed by Hwang et al. [58], is one of the most common and widely used methods for multi-criteria decision-making. This is based on the distances of each of the alternatives to the ideal solutions, both positive and negative [59]. The positive ideal solution maximizes the benefit response and minimizes the cost response, while the negative ideal solution is the other way around. Therefore, the best alternative will be the one closest to the ideal positive solution and furthest from the ideal negative solution. The steps of the TOPSIS method are described below:

Step 1: Establish the decision-making matrix, which has the following form $X = [$

$x_{ij}] = m \times n$, as in the WASPAS method.

Step 2: Normalize the decision matrix with the following equation:

$$r_{ij} = \frac{X_{ij}}{\sqrt{\sum_{j=1}^{n} X_{ij}}}, i = 1,2,3,\ldots,n; j = 1,2,3,\ldots,m \tag{14}$$

where $r_{ij}$ is the normalized criteria rating.

Step 3: Obtain the weighted normalized decision matrix, with the following equation:

$$\left[v_{ij}\right] = [w_j r_{ij}] \tag{15}$$

$$\sum_{j=1}^{n} w_j = 1 \tag{16}$$

where $[v_{ij}]$ is the weighted normalized matrix and $w_j$ is the weightage of each criterion.

Step 4: Calculate the positive (PIS) and negative ideal solutions (NIS). For this purpose, the following equations are used:

$$V^+ = (v_1^+, v_2^+, v_3^+, \ldots v_n^+) = \left\{ \left( \underset{i}{max} v_{ij} \forall j \in J \right) | \left( \underset{i}{min} v_{ij} \forall j \in J' \right) \right\} \tag{17}$$

$$V^- = (v_1^-, v_2^-, v_3^-, \ldots v_n^-) = \left\{ \left( \underset{i}{min} v_{ij} \forall j \in J \right) | \left( \underset{i}{max} v_{ij} \forall j \in J' \right) \right\} \tag{18}$$

where $J$ is a beneficial criterion and $J'$ is a non-beneficial criterion.

Step 5: Calculate the Euclidean distance of each alternative to the positive ideal solution and to the negative ideal solution, using the following equations:

$$d_i^+ = \sqrt{\sum_{j=1}^{n} \left(v_{ij} - v_j^+\right)^2} \tag{19}$$

$$d_i^- = \sqrt{\sum_{j=1}^{n} \left(v_{ij} - v_j^-\right)^2} \tag{20}$$

Step 6: Calculate the relative closeness of each alternative to the ideal solution, using the following equation:

$$RC_i = \frac{d_i^-}{d_i^+ + d_i^-} \tag{21}$$

#### 2.7.3 AHP method

When using multi-criteria decision-making methods, calculating and assigning the relative weights of the criteria is an important part of the process to obtain an optimal result. For this purpose, this study applied the AHP method [60], based on subjective weighting, which allows obtaining information based on the knowledge and experience of experts. Criteria weighting was performed using pairwise comparison matrices that are based on the experts judgement, for which a survey is designed that is sent individually to each expert to collect their opinion. The data collected per each expert was converted into a pairwise comparison matrix form $[X] = [x_{ij}] = n \times n$, where $n$ corresponds to the number of assessment criteria considered and satisfying the expression $x_{jk} \times x_{kj} = 1$, where $x_{jk}$ is one of the entries of the matrix and $x_{kj}$ its reciprocal value. The numerical scale from one to nine was used to measure the relative importance between two criteria.

The consistency of each judgment was checked by calculating the Consistency Ratio (CR):

$$C.R = \frac{C.I}{R.C.I} < 0.2 \tag{22}$$

R.C.I. is the Random Consistency Index, whose values are defined in Table 6. C.I. is the consistency index, which is calculated with the following equation:

$$C.I. = \frac{\lambda_{max} - 1}{n - 1} \tag{23}$$

where $\lambda_{max}$ is the maximum eigenvalue of the matrix, and when $\lambda_{max} = n$ the matrix is consistent and starts to be inconsistent when this value decreases.

## 3 Results and discussion

### 3.1 Rheological tests

The yield stress values of the different mixtures range between 100 and 700 Pa and those of viscosity between 15 and 25 Pa*s. Table 7 shows the values of yield stress, viscosity, and printability index.

In relation to yield stress, it has been found that both fiber type and fiber content significantly affect yield stress (Table 8 (a)). These findings are based on an ANOVA test to identify which of these 3 input variables (fiber type, fiber length, fiber dosage) have a significant influence on the response (yield stress). In the case of fiber type the $p$-value was 0.005 and for fiber dosage the $p$-value was 0.000. Fiber length did not have a significant influence over yield stress ($p = 0.608$). Regarding viscosity, the same ANOVA test was carried out finding that the three variables had significant influence over the viscosity, resulting in $p$-values of 0.001, 0.017, and 0.003 for fiber type, fiber length, and fiber dosage, respectively. For the printability index, defined as the yield stress*viscosity, the ANOVA test detects significant influence on fiber type ($p$-value:0.000) and fiber dosage ($p$-value:0.001), but not on the fiber length ($p$-value:0.160).

As for the yield stress values, it can be observed that they increase as the fiber content increases in all the mixtures analyzed (Table 8 (b)). Therefore, the force to initiate flow that the printer endless screw has to perform becomes higher as the fiber content increases. This was also observed in the laboratory during the preliminary printing trials, since as the fiber content increased, the mixtures printed in worse conditions, in some cases beginning to cut or to remain blocked in the nozzle. The higher fiber contents that were analyzed and of which the rheological analysis was carried out were at the limit that allowed the mixtures to print correctly, without the problems mentioned above. Regarding the viscosity value, this has a tendency opposite to that of yield stress, since as the fiber content increases, the mixtures reduce the viscosity value. These variations in viscosity are not as noticeable as in the case of yield stress for each type of fiber. As a result, the printability index increases with the increase of dosage, as it can be seen in the regression model generated.

**Table 6** Random Consistency Index (R.C.I.) values

| Matrix size ($n$) | 2 | 3 | 4 | 5 | 6 | 7 | 8 | 9 | 10 |
|---|---|---|---|---|---|---|---|---|---|
| R.C.I. | 0.00 | 0.58 | 0.90 | 1.12 | 1.24 | 1.32 | 1.41 | 1.45 | 1.49 |

**Table 7** Rheological test results and printability index

| Material | Fiber length (mm) | Fiber percent (%) | Yield stress (Pa) | Viscosity (Pa*s) | Printability index: yield stress (Pa)*viscosity (Pa*s) |
|---|---|---|---|---|---|
| Aramid | 30 | 0.05 | 339.71 | 22.64 | 7691.03 |
| | | 0.075 | 445.67 | 21.83 | 9728.98 |
| | | 0.1 | 535.59 | 14.95 | 8007.07 |
| | 20 | 0.05 | 250.33 | 24.11 | 6035.46 |
| | | 0.1 | 325.87 | 22.54 | 7345.11 |
| | | 0.2 | 473.98 | 22.11 | 10479.70 |
| | 6 | 0.05 | 201.42 | 20.56 | 4141.20 |
| | | 0.075 | 247.65 | 18.97 | 4697.92 |
| | | 0.1 | 282.57 | 17.91 | 5060.83 |
| | 12 | 0.05 | 113.99 | 17.64 | 5060.83 |
| | | 0.075 | 591.7 | 15.88 | 9396.20 |
| Carbon | 25 | 0.05 | 204.2 | 22.73 | 4641.47 |
| | | 0.075 | 358.03 | 21.15 | 7572.33 |
| | | 0.1 | 491.63 | 19.23 | 9454.04 |
| | 6 | 0.05 | 199.05 | 22.67 | 4512.46 |
| | | 0.1 | 287.39 | 19.03 | 5469.03 |
| | | 0.2 | 451.01 | 18.72 | 8442.91 |
| Cellulose | 6 | 0.05 | 246.64 | 19.56 | 4824.28 |
| | | 0.075 | 426.86 | 18.47 | 7884.10 |
| | | 0.1 | 638.25 | 17.23 | 10997.05 |
| | 20 | 0.05 | 291.03 | 24.51 | 7133.15 |
| | | 0.075 | 421.99 | 21.14 | 8920.87 |
| | | 0.1 | 620.89 | 17.57 | 10909.04 |
| Glass | 13.1 | 0.1 | 185.01 | 23.97 | 4434.69 |
| | | 0.2 | 423.45 | 20.15 | 8532.52 |
| | | 0.3 | 571.77 | 17.96 | 10268.99 |
| Zylon | 6 | 0.05 | 247.46 | 24.96 | 6176.60 |
| | | 0.075 | 351.37 | 24.37 | 8562.89 |
| | | 0.1 | 472.49 | 23.28 | 10999.57 |
| Textile | 20 | 0.05 | 495.36 | 24.89 | 12329.51 |
| | | 0.075 | 596.38 | 24.56 | 14647.09 |
| | | 0.1 | 698.36 | 23.98 | 16746.67 |
| Polypropylene | 6 | 0.05 | 374.92 | 18.34 | 6876.03 |
| | | 0.075 | 425.76 | 18.21 | 7753.09 |
| | | 0.1 | 495.95 | 17.85 | 8852.71 |
| Control | | | 447.23 | 11.58 | 5178.92 |

## 3.2 Mechanical tests

Figure 5 (top) shows the flexural strength results obtained at 28 days for the mixtures with the different types and percentages of fibers. Values ranged from 9.49 to 11.70 MPa, while the control sample (no fibers) achieved 9.04 MPa, showing that flexural strength significantly increases with the addition of fibers, reaching a maximum increase of 30% with zylon fibers. Other fibers, such as carbon, glass, or polypropylene, also obtained high strength increases. On the other hand, recycled textile fibers were the worst performers in terms of strength.

Regarding the flexural strength values, it can be concluded that the best results have been obtained with the incorporation of 1% of zylon fibers, with an increase over the control mixture of 30%. This was followed by mixtures incorporating 0.1% of carbon fibers, both 6 and 25 mm in length, which achieved increases of 24%. In addition, both glass fibers with a content of 0.3% and polypropylene fibers with 0.05% have reached increases exceeding 20%. Finally,

**Table 8** Correlation between rheological parameters vs. fiber type, length, and dosage

(a) Coefficients and *p*-values of an ANOVA test

| | Yield stress | | Viscosity | | Printability index[1] | |
|---|---|---|---|---|---|---|
| Terms | *p*-value | Significance ($p<0.05$) | *p*-value | Significance ($p<0.05$) | *p*-value | Significance ($p<0.05$) |
| Type | 0.005 | Yes | 0.001 | Yes | 0.000 | Yes |
| Length (mm) | 0.608 | No | 0.017 | Yes | 0.160 | No |
| Dosage (%) | 0.000 | Yes | 0.003 | Yes | 0.001 | Yes |

(b) Regression models and determination coefficients

| Dependant variable | Formulae | Determination coefficients |
|---|---|---|
| Yield stress (Pa) | 291.9 + 1026*dosage (%) | 19.70% |
| Viscosity (Pa*s) | 22.341 − 16.77*dosage (%) | 14.21% |
| Printability index ($Pa^2$*s) | 6754 + 12,993*dosage (%) | 7.43% |

[1]Printability index = yield stress*viscosity

textile fibers with any of their contents are the worst performers, as they did not achieve an increase of 10%.

Hambach [61] performed a flexural test in 3D-printed samples reinforced with carbon fibers by applying a force in the normal direction of printing planes, reporting 13.9 MPa of flexural strength vs 11.4 MPa of control samples without fibers, which represents a 22% increment. The 3D printing pattern used were lays where the 3D-printed filaments direction was changed 90° degrees between one lay and the next one (what he called "Print path B"), since it is a quite common practice in 3D printing. These results are aligned with the results obtained in this paper for carbon fibers, which prove, at a certain extent, that assessing flexural strength on cast samples for 3D printing applications could be an acceptable approach to save testing time if printing patterns are changed 90° between layers.

The results of the compressive strength at 28 days of the different mixes analyzed in this study are shown in Fig. 5 (bottom). The compressive strength values obtained in the reference sample were 52.5 MPa and with the incorporation of the fibers the ranges varied between 49.38 and 56.92 MPa, yielding increments ranging from − 6 to 8%. Therefore, fibers in reinforced mortar show no clear advantage or disadvantage, as pointed out by different authors and summarized in [45].

In terms of the influence on length, dosage, strength, and elastic modulus of the fibers in relation to the flexural strength, an ANOVA test was carried out to find out correlations and only the elastic modulus of the fibers has a significant influence on the flexural strength with *p*-values of 0.514 (length), 0.334 (strength), 0.904 (dosage), and 0.015 (elastic modulus). Results of mortars including textile fibers and polypropylene fibers were omitted from the ANOVA since the manufacturers did not provide the values of fiber strength and/or elastic modulus.

In Table 9, the ANOVA test results and the regression model generated for the flexural strength are summarized. This finding, the correlation between flexural strength and elastic modulus of fibers, has been reported by [62]. The lack of correlation with fiber length and dosage could be due to the fact that these factors could be beneficial or disadvantegous depending on how homogenous is the mixing process. For example, sometimes, large amounts and/or very long fibers could make the batch not to as homogenous as desired, producing voids that might affect flexural strength. In other occasions, on the contrary, large amounts of fibers and/or length could have the opposite effect, if mixing is homogeneous, might produce more resistant mortars. Alternatively, other factors from what we have no data, like the mortar-fiber bonding, could also have an influence, as mentioned in [62].

Finally, in order to verify that these increases in flexural strength with the incorporation of fibers are indeed significant, a statistical analysis was carried out. The results obtained are shown in Table 10, where it can be seen that all the *p*-values obtained were lower than 0.05. These indicate that the incorporation of fibers significantly affects the increase in flexural strength. Only in the case of the 20-mm-long aramid fibers with a content of 0.3%, it was observed that this *p*-value was 0.326, not meeting the requirement to significantly affect. These fibers were the worst performers in flexural strength with an increase of only 5%. In addition, the statistical analysis of the compressive strength results was also carried out, proving that the results obtained for the *p*-value were greater than 0.05, demonstrating that the fibers do not significantly influence in this case.

With these results obtained in the statistical analysis, it was demonstrated that the fibers in the case of compressive strength had no major effect (see Table 10), but on the contrary, significantly impacted the flexural strength, so this was selected as a criterion for the MCMDA analysis.

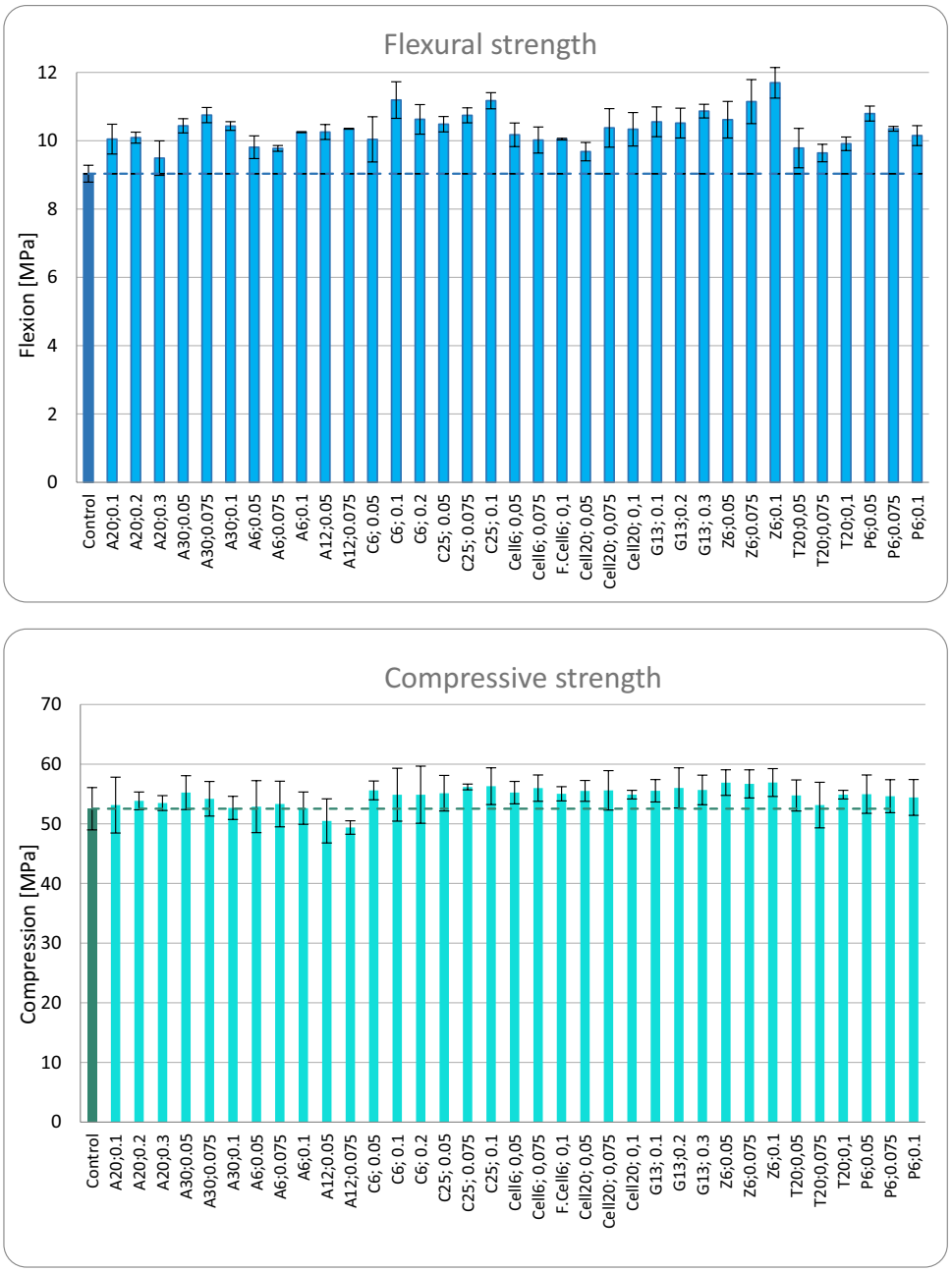


**Fig. 5** Average of flexural (top) and compressive (bottom) strength at 28 days, standard deviation about mean is represented by the bars

**Table 9** Correlation between flexural strength vs fiber length, strength, elastic modulus, and dosage

| (a) Coefficients and *p*-values of an ANOVA test | | |
|---|---|---|
| | Flexural strength | |
| Terms | *p*-value | Significance ($p < 0.05$) |
| Length (mm) | 0.514 | No |
| Strength (MPa) | 0.334 | No |
| Elastic modulus (GPa) | 0.015 | Yes |
| Dosage (%) | 0.904 | No |
| (b) Regression model | | |
| Dependant variable | Formulae | Determination coefficients |
| Flexural strength (MPa) | 10.041 + 0.00334*elastic modulus (GPa) | 41.73% |

**Table 10** Results of statistical analysis of flexural and compressive strength as compared to control mixture

| Mixture | | Flexural strength (MPa) | | | Compressive strength (MPa) | | |
|---|---|---|---|---|---|---|---|
| | | Test result | *p*-value | Significance | Test result | *p*-value | Significance |
| Control | | 9.04 | | | 52.53 | | |
| Aramid | A20;0.1 | 10.05 | 0.048 | Yes | 53.14 | 0.850 | No |
| | A20;0.2 | 10.09 | 0.008 | Yes | 53.84 | 0.618 | No |
| | A20;0.3 | 9.49 | 0.326 | No | 53.48 | 0.714 | No |
| | A30;0.05 | 10.44 | 0.008 | Yes | 55.23 | 0.396 | No |
| | A30;0.075 | 10.75 | 0.006 | Yes | 54.20 | 0.553 | No |
| | A30;0.1 | 10.43 | 0.045 | Yes | 52.67 | 0.883 | No |
| | A6;0.05 | 9.81 | 0.030 | Yes | 52.88 | 0.917 | No |
| | A6;0.075 | 9.78 | 0.047 | Yes | 53.32 | 0.931 | No |
| | A6;0.1 | 10.25 | 0.001 | Yes | 52.63 | 0.970 | No |
| | A12;0.05 | 10.26 | 0.007 | Yes | 50.49 | 0.487 | No |
| | A12;0.075 | 10.35 | 0.000 | Yes | 49.38 | 0.383 | No |
| Carbon | C6; 0.05 | 10.04 | 0.036 | Yes | 55.60 | 0.273 | No |
| | C6; 0.1 | 11.19 | 0.020 | Yes | 54.88 | 0.117 | No |
| | C6; 0.2 | 10.63 | 0.033 | Yes | 54.88 | 0.541 | No |
| | C25; 0.05 | 10.48 | 0.009 | Yes | 55.13 | 0.451 | No |
| | C25; 0.075 | 10.74 | 0.008 | Yes | 56.18 | 0.284 | No |
| | C25; 0.1 | 11.17 | 0.004 | Yes | 56.31 | 0.349 | No |
| Cellulose | Cell6; 0.05 | 10.17 | 0.031 | Yes | 55.23 | 0.378 | No |
| | Cell6; 0.075 | 10.02 | 0.026 | Yes | 55.98 | 0.403 | No |
| | Cell;6; 0.1 | 10.05 | 0.001 | Yes | 55.03 | 0.352 | No |
| | Cell20; 0.05 | 9.68 | 0.041 | Yes | 55.52 | 0.286 | No |
| | Cell20; 0.075 | 10.38 | 0.002 | Yes | 55.61 | 0.296 | No |
| | Cell20; 0.1 | 10.34 | 0.002 | Yes | 54.89 | 0.371 | No |
| Glass | G13; 0.1 | 10.55 | 0.027 | Yes | 55.54 | 0.287 | No |
| | G13;0.2 | 10.52 | 0.029 | Yes | 56.02 | 0.270 | No |
| | G13; 0.3 | 10.87 | 0.004 | Yes | 55.68 | 0.245 | No |
| Zylon | Z6;0.05 | 10.62 | 0.046 | Yes | 56.91 | 0.129 | No |
| | Z6;0.075 | 11.15 | 0.022 | Yes | 56.69 | 0.170 | No |
| | Z6;0.1 | 11.70 | 0.011 | Yes | 56.92 | 0.141 | No |
| Textile | T20;0.05 | 9.79 | 0.008 | Yes | 54.75 | 0.424 | No |
| | T20;0.075 | 9.64 | 0.040 | Yes | 53.14 | 0.756 | No |
| | T20;0.1 | 9.91 | 0.011 | Yes | 54.89 | 0.371 | No |
| Polypropylene | P6;0.05 | 10.80 | 0.048 | Yes | 54.97 | 0.462 | No |
| | P6;0.075 | 10.35 | 0.042 | Yes | 54.63 | 0.589 | No |
| | P6;0.1 | 10.15 | 0.022 | Yes | 54.42 | 0.611 | No |

### 3.3 Life cycle assessment (LCA)

As the last criterion for the MCDM analysis, the environmental impact was selected. The results obtained through the EF 3.0 method of the mixtures with the different types and percentages of fibers are shown in Table 11. The results obtained were quite similar for the different dosages, since they only modify the type and percentage of fibers, which account for a very small amount of the mixtures, as it can be seen in Fig. 6 (for the particular case of polypropylene fibers). Although these variations are not very large, it can be observed that the textile fibers get the worst results in the LCA analysis, followed by the aramid fibers. In contrast, cellulose and polypropylene fibers were the best performers. These results of the indicators for each category have been converted, by normalization and weighting, into single results for each of the mixtures (Fig. 7), which can be entered in the MCMDA.

**Table 11** Environmental impact (EF 3.0 method)

| Impact | Control | 0.05% | | | | | |
|---|---|---|---|---|---|---|---|
| | | Aramid | Carbon | Cellulose | Polyprop | Textile | Zylon |
| Climate change | 104.31774 | 110.5177 | 106.7432 | 104.477 | 105.5053 | 104.329 | 106.1145 |
| Ozone depletion | 6.50E-06 | 6.50E-06 | 6.54E-06 | 6.52E-06 | 6.52E-06 | 6.50E-06 | 8.85E-06 |
| Ionizing radiation | 15.152888 | 15.44139 | 1.52E + 01 | 1.52E + 01 | 1.52E + 01 | 1.52E + 01 | 1.52E + 01 |
| Photochemical ozone formation | 0.2894802 | 0.29803 | 0.295877 | 0.29028 | 0.2933577 | 0.28956 | 0.298589 |
| Particulate matter | 3.11E-06 | 3.19E-06 | 3.21E-06 | 3.13E-06 | 3.15E-06 | 3.11E-06 | 3.51E-06 |
| Human toxicity, non-cancer | 9.05E-07 | 1.07E-06 | 9.12E-07 | 9.08E-07 | 9.12E-07 | 9.05E-07 | 9.63E-07 |
| Human toxicity, cancer | 3.27E-08 | 5.92E-08 | 3.32E-08 | 3.29E-08 | 3.30E-08 | 3.27E-08 | 3.64E-08 |
| Acidification | 0.4886356 | 0.498986 | 4.97E-01 | 4.90E-01 | 4.93E-01 | 4.89E-01 | 5.49E-01 |
| Eutrophication, freshwater | 0.0252474 | 0.025262 | 0.025388 | 0.0253 | 0.0254466 | 0.02525 | 0.025833 |
| Eutrophication, marine | 0.0976087 | 0.100264 | 0.099053 | 0.09787 | 0.0985082 | 0.09763 | 0.101623 |
| Eutrophication, terrestrial | 1.0865675 | 1.114968 | 1.100644 | 1.08933 | 1.0961126 | 1.08685 | 1.107859 |
| Ecotoxicity, freshwater | 2938.7667 | 2939.362 | 2963.217 | 2945.32 | 2950.7697 | 2938.91 | 3127.335 |
| Land use | 364.36805 | 396.6181 | 365.2225 | 365.087 | 366.00726 | 364.448 | 377.8594 |
| Water use | 24.837465 | 24.79982 | 26.08184 | 24.8707 | 25.310495 | 24.8381 | 26.39968 |
| Resource use, fossils | 1032.4511 | 1142.451 | 1078.728 | 1034.31 | 1070.1224 | 1032.62 | 1061.673 |
| Resource use, minerals and metals | 0.0005849 | 0.000586 | 0.000586 | 0.00059 | 0.0005922 | 0.00058 | 0.000622 |

| Impact | Control | 0.075% | | | | | | 0.1% | | |
|---|---|---|---|---|---|---|---|---|---|---|
| | | Aramid | Carbon | Cellulose | Polyprop | Textile | Zylon | Aramid | Carbon | Cellulose |
| Climate change | 104.31774 | 113.6177 | 107.956 | 104.5559 | 106.0991 | 104.334 | 107.013 | 116.718 | 109.169 | 104.6353 |
| Ozone depletion | 6.50E-06 | 6.50E-06 | 6.57E-06 | 6.52E-06 | 6.54E-06 | 6.51E-06 | 1.00E-05 | 6.50E-06 | 6.59E-06 | 6.53E-06 |
| Ionizing radiation | 15.152888 | 15.58564 | 15.1709 | 15.17195 | 15.19831 | 15.1543 | 15.2942 | 15.7299 | 15.1769 | 15.1783 |
| Photochemical ozone formation | 0.2894802 | 0.302305 | 0.29908 | 0.290678 | 0.295296 | 0.2896 | 0.30314 | 0.30658 | 0.30227 | 0.291077 |
| Particulate matter | 3.11E-06 | 3.23E-06 | 3.25E-06 | 3.13E-06 | 3.17E-06 | 3.11E-06 | 3.70E-06 | 3.27E-06 | 3.30E-06 | 3.14E-06 |
| Human toxicity, non-cancer | 9.05E-07 | 1.16E-06 | 9.15E-07 | 9.10E-07 | 9.15E-07 | 9.05E-07 | 9.92E-07 | 1.24E-06 | 9.19E-07 | 9.11E-07 |
| Human toxicity, cancer | 3.27E-08 | 7.24E-08 | 3.35E-08 | 3.30E-08 | 3.32E-08 | 3.27E-08 | 3.82E-08 | 8.56E-08 | 3.37E-08 | 3.31E-08 |
| Acidification | 0.4886356 | 0.504161 | 0.50072 | 0.490403 | 0.495543 | 0.48874 | 0.57933 | 0.50934 | 0.50475 | 0.490992 |
| Eutrophication, freshwater | 0.0252474 | 0.02527 | 0.02546 | 0.025322 | 0.025546 | 0.02525 | 0.02613 | 0.02528 | 0.02553 | 0.025347 |
| Eutrophication, marine | 0.0976087 | 0.101591 | 0.09977 | 0.098008 | 0.098958 | 0.09765 | 0.10363 | 0.10292 | 0.1005 | 0.098141 |
| Eutrophication, terrestrial | 1.0865675 | 1.129168 | 1.10768 | 1.090713 | 1.100885 | 1.08699 | 1.1185 | 1.14337 | 1.11472 | 1.092095 |
| Ecotoxicity, freshwater | 2938.7667 | 2939.659 | 2975.44 | 2948.595 | 2956.771 | 2938.98 | 3221.62 | 2939.96 | 2987.67 | 2951.872 |
| Land use | 364.36805 | 412.7431 | 365.65 | 365.4462 | 366.8269 | 364.489 | 384.605 | 428.868 | 366.077 | 365.8056 |
| Water use | 24.837465 | 24.78099 | 26.704 | 24.88726 | 25.54701 | 24.8384 | 27.1808 | 24.7622 | 27.3262 | 24.90385 |
| Resource use, fossils | 1032.4511 | 1197.451 | 1101.87 | 1035.234 | 1088.958 | 1032.7 | 1076.28 | 1252.45 | 1125 | 1036.161 |
| Resource use, minerals and metals | 0.0005849 | 0.000587 | 0.00059 | 0.000587 | 0.000596 | 0.00059 | 0.00064 | 0.00059 | 0.00059 | 0.000588 |

| Impact | Control | 0.1% | | | | 0.2% | | | 0.3% | |
|---|---|---|---|---|---|---|---|---|---|---|
| | | Glass | Polyprop | Textile | Zylon | Glass | Carbon | Aramid | Glass | Aramid |
| Climate change | 104.31774 | 106.8171 | 106.6929 | 104.34 | 107.9112 | 109.316 | 114.02 | 129.118 | 111.816 | 141.5177 |
| Ozone depletion | 6.50E-06 | 6.66E-06 | 6.55E-06 | 6.51E-06 | 1.12E-05 | 6.82E-06 | 6.67E-06 | 6.50E-06 | 6.98E-06 | 6.50E-06 |
| Ionizing radiation | 15.152888 | 15.38674 | 15.21346 | 15.1548 | 15.34125 | 15.6206 | 15.201 | 16.3069 | 15.8544 | 16.88389 |
| Photochemical ozone formation | 0.2894802 | 0.300931 | 0.297235 | 0.28964 | 0.307698 | 0.31238 | 0.31507 | 0.32368 | 0.32383 | 0.34078 |
| Particulate matter | 3.11E-06 | 3.25E-06 | 3.19E-06 | 3.11E-06 | 3.90E-06 | 3.39E-06 | 3.50E-06 | 3.43E-06 | 3.53E-06 | 3.59E-06 |
| Human toxicity, non-cancer | 9.05E-07 | 1.04E-06 | 9.18E-07 | 9.05E-07 | 1.02E-06 | 1.17E-06 | 9.33E-07 | 1.58E-06 | 1.30E-06 | 1.91E-06 |
| Human toxicity, cancer | 3.27E-08 | 3.51E-08 | 3.34E-08 | 3.28E-08 | 4.01E-08 | 3.75E-08 | 3.47E-08 | 1.39E-07 | 3.98E-08 | 1.91E-07 |
| Acidification | 0.4886356 | 0.507197 | 0.497845 | 0.48877 | 0.609558 | 0.52576 | 0.52086 | 0.53004 | 0.54432 | 0.550736 |
| Eutrophication, freshwater | 0.0252474 | 0.025982 | 0.025646 | 0.02525 | 0.026418 | 0.02672 | 0.02581 | 0.02531 | 0.02745 | 0.025336 |
| Eutrophication, marine | 0.0976087 | 0.1015 | 0.099408 | 0.09766 | 0.105637 | 0.10539 | 0.10338 | 0.10823 | 0.10928 | 0.113539 |

Table 11 (continued)

| Impact | Control | 0.1% | | | | 0.2% | | | 0.3% | |
|---|---|---|---|---|---|---|---|---|---|---|
| | | Glass | Polyprop | Textile | Zylon | Glass | Carbon | Aramid | Glass | Aramid |
| Eutrophication, terrestrial | 1.0865675 | 1.127817 | 1.105658 | 1.08713 | 1.12915 | 1.16907 | 1.14287 | 1.20017 | 1.21031 | 1.256968 |
| Ecotoxicity, freshwater | 2938.7667 | 2976.867 | 2962.773 | 2939.05 | 3315.904 | 3014.97 | 3036.57 | 2941.15 | 3053.07 | 2942.337 |
| Land use | 364.36805 | 371.699 | 367.6465 | 364.529 | 391.3507 | 379.03 | 367.786 | 493.368 | 386.361 | 557.8681 |
| Water use | 24.837465 | 25.39102 | 25.78352 | 24.8387 | 27.96189 | 25.9446 | 29.815 | 24.6869 | 26.4981 | 24.61157 |
| Resource use, fossils | 1032.4511 | 1065.413 | 1107.794 | 1032.78 | 1090.895 | 1098.38 | 1217.56 | 1472.45 | 1131.34 | 1692.451 |
| Resource use, minerals and metals | 0.0005849 | 0.000606 | 0.0006 | 0.00059 | 0.000658 | 0.00063 | 0.00059 | 0.00059 | 0.00065 | 0.000592 |

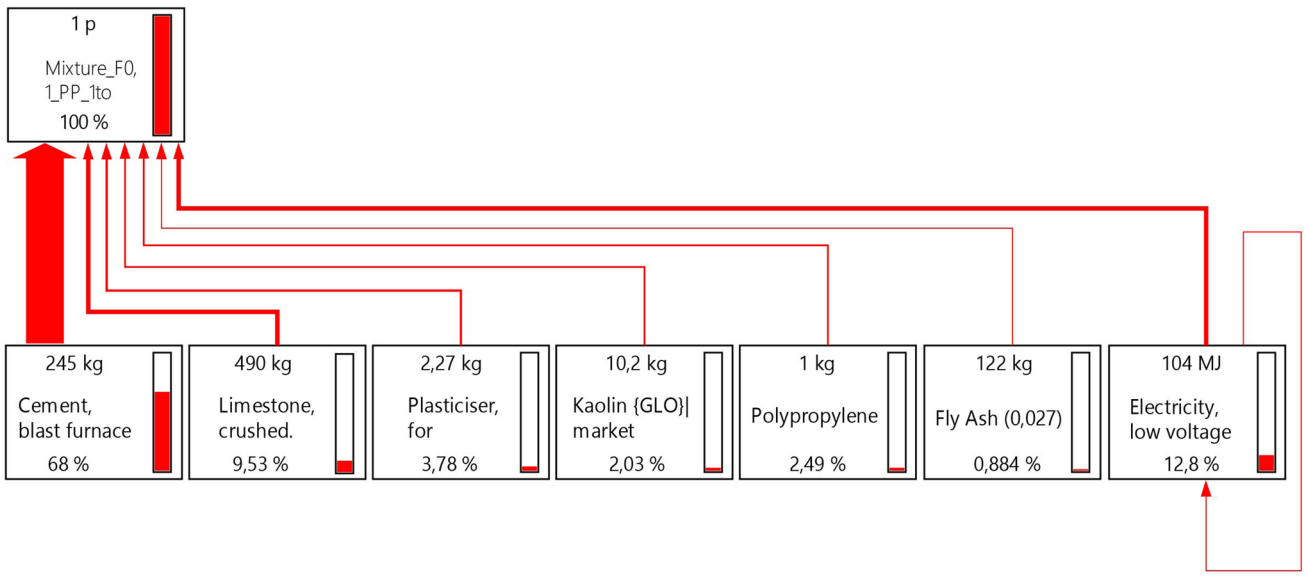


**Fig. 6** Contribution of unit processes to the total impact for the mixture with 0.1% polypropylene fiber

**Fig. 7** LCA points of each mixture

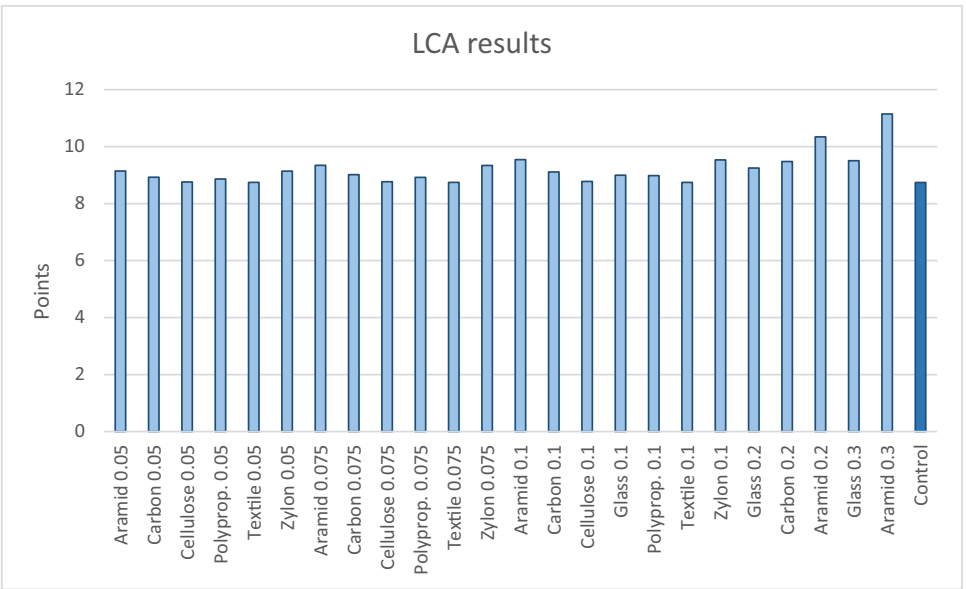

**Table 12** Cost per tonne for each mixture depending on the percentage of fiber (in weight) added

| Aramid | | Carbon | | Cellulose | | Glass | | Zylon | | Textile | | Polypropylene | |
|---|---|---|---|---|---|---|---|---|---|---|---|---|---|
| % | €/t | % | €/t | % | €/t | % | €/t | % | €/t | % | €/t | % | €/t |
| 0.05 | 68.63 | 0.05 | 62.13 | 0.05 | 49.81 | 0.1 | 52.02 | 0.05 | 149.13 | 0.05 | 49.13 | 0.05 | 60.73 |
| 0.075 | 78.37 | 0.075 | 68.62 | 0.075 | 50.13 | 0.2 | 60.66 | 0.075 | 199.12 | 0.075 | 49.13 | 0.075 | 66.52 |
| 0.1 | 88.11 | 0.1 | 75.11 | 0.1 | 50.46 | 0.3 | 66.41 | 0.1 | 249.11 | 0.1 | 49.13 | 0.1 | 72.31 |
| 0.2 | 127.06 | 0.2 | 101.06 | | | | | | | | | | |
| 0.3 | 166.01 | | | | | | | | | | | | |

## 3.4 Cost

Table 12 shows the cost of each of the 36 mixes together with the control (no fibers). The cost of fibers has a fairly high weight in the total mix and is highly variable depending on the type. This is why the costs of the different mixtures vary so much, going from 49.13 €/t for textile mixes to 249.11€/t for mixes incorporating the highest content of zylon.

## 3.5 Multi-criteria decision-making analysis (MCDMA)

The weighing factors are shown in Table 13 while the values of the 4 indicators for the decision matrix are summarized in Table 14.

In relation to the weighing factors, in the AHP method, printability criteria was the highest, followed by mechanical resistance, environmental, and economic criteria. A second scenario was proposed in which equal weight is assigned to each of the criteria (25%).

The classification of the mixtures was carried out with the two proposed multi-criteria analysis methods, WASPAS and TOPSIS, to verify that the results with both methods order the 36 alternatives (35 + control) in a similar way. The ranking of the two scenarios, with the two multi-criteria analysis methods, is shown in Fig. 8. The CC and JPS score values range between 0 and 1 for the TOPSIS and WASPAS methods, respectively, with the best alternatives having the highest values.

The results obtained with both methods and in the two scenarios were very similar showing the same mixtures in the first and last places. The dosages were G13;0.1, Cell6;0.05, and C25;0.05. This is due to the fact that these dosages present good increases in resistance, which, although not the highest, oscillate between 15 and 20%, and have good printability values. Also, since these are the dosages that incorporate the lowest percentages of fibers and the type of fibers are also more economical, they have the lowest costs, since fibers constitute a very important part of the total price of the mixture. On the other hand, it has been obtained that the dosages incorporating both zylon, aramid of 20 mm, and textile fibers are the ones presenting the worst results. In the first case, in spite of presenting the best values of increase in flexural strength, these mixtures present very high costs in comparison with the rest of the fibers. In the second case, in addition to the high prices of the mixtures, they show some of the lowest increases in flexural strength. Finally, the textile fibers are also in the last positions, since they present the lowest increases in flexural strength and the worst printability values, as it could also be verified in the laboratory, since they were the fibers that presented the most problems when printing.

In addition, it is also obtained that the LCA presents very similar values in all the dosages because the only difference they present is the type of fibers used and in very low quantities. Therefore, both in Scenario 1 (weight, 21.83%) and Scenario 2 (weight, 25%), the results of the LCA have a very low impact. Furthermore, the increase of fiber content in all types of dosages produces an increase in the cost and a decrease in the workability (low workability is related to a high printability index: yield stress*viscosity), so that the mixtures with lower fiber content usually present the best results in the analysis, since it is difficult for the increase in flexural strength to be high enough as to compensate with the other two criteria punctuation.

In summary, mortars with glass, cellulose, and carbon fibers are those that occupy the first positions in the ranking. Those incorporating zylon, aramid of 20 mm, and textile fibers occupy the last positions. Control samples (no fibers) rank in a relatively good position, between 4 (Scenario 2, WASPAS) to 10 (Scenario 1, TOPSIS), proving that that the use of certain type of fibers would be even worse that not using any fibers.

**Table 13** Weights assigned to each criterion

| | Printability index | Flexural strength | Cost | LCA |
|---|---|---|---|---|
| Scenario 1 (AHP method) | 0.3814 | 0.2717 | 0.1286 | 0.2183 |
| Scenario 2 (equal weights) | 0.25 | 0.25 | 0.25 | 0.25 |

**Table 14** Input values for the MCDMA decision matrix

| | Non-beneficial criteria | Beneficial criteria | Non-beneficial criteria | Non-beneficial criteria |
|---|---|---|---|---|
| | Printability index (Pa^2*s) | Flexural strenght (MPa) | Cost (€/t) | LCA (Points) |
| Control | 5178.92 | 9.04 | 49.13 | 8.74 |
| A20; 0.1 | 7691.03 | 10.05 | 88.11 | 9.54 |
| A20; 0.2 | 9728.98 | 10.09 | 127.06 | 10.34 |
| A20; 0.3 | 8007.07 | 9.49 | 166.01 | 11.14 |
| A30; 0.05 | 6035.46 | 10.44 | 68.63 | 9.14 |
| A30; 0.075 | 7345.11 | 10.75 | 78.37 | 9.34 |
| A30; 0.1 | 10,479.70 | 10.43 | 88.11 | 9.54 |
| A6; 0.05 | 4141.20 | 9.81 | 68.63 | 9.14 |
| A6; 0.075 | 4697.92 | 9.78 | 78.37 | 9.34 |
| A6; 0.1 | 5060.83 | 10.25 | 88.11 | 9.54 |
| A12; 0.05 | 5060.83 | 10.26 | 68.63 | 9.14 |
| A12; 0.075 | 9396.20 | 10.35 | 78.37 | 9.34 |
| C6; 0.05 | 4641.47 | 10.04 | 62.13 | 8.93 |
| C6; 0.1 | 7572.33 | 11.19 | 75.11 | 9.11 |
| C6; 0.2 | 9454.04 | 10.63 | 101.06 | 9.48 |
| C25; 0.05 | 4512.46 | 10.48 | 62.13 | 8.93 |
| C25; 0.075 | 5469.03 | 10.74 | 68.62 | 9.02 |
| C25; 0.1 | 8442.91 | 11.17 | 75.11 | 9.11 |
| Cell6; 0.05 | 4824.28 | 10.17 | 49.81 | 8.76 |
| Cell6; 0.075 | 7884.10 | 10.02 | 50.13 | 8.77 |
| Cell6; 0.1 | 10,997.05 | 10.05 | 50.46 | 8.78 |
| Cell20; 0.05 | 7133.15 | 9.68 | 49.81 | 8.76 |
| Cell20; 0.075 | 8920.87 | 10.38 | 50.13 | 8.77 |
| Cell20; 0.1 | 10,909.04 | 10.34 | 50.46 | 8.78 |
| G13; 0.1 | 4434.69 | 10.55 | 52.02 | 8.99 |
| G13;0.2 | 8532.52 | 10.52 | 60.66 | 9.25 |
| G13; 0.3 | 10,268.99 | 10.87 | 66.41 | 9.50 |
| Z6; 0.05 | 6176.60 | 10.62 | 149.13 | 9.14 |
| Z6; 0.075 | 8562.89 | 11.15 | 199.12 | 9.34 |
| Z6; 0.1 | 10,999.57 | 11.70 | 249.11 | 9.54 |
| T20; 0.05 | 12,329.51 | 9.79 | 49.13 | 8.74 |
| T20; 0.075 | 14,647.09 | 9.64 | 49.13 | 8.74 |
| T20; 0.1 | 16,746.67 | 9.91 | 49.13 | 8.74 |
| P6; 0.05 | 6876.03 | 10.80 | 60.73 | 8.86 |
| P6; 0.075 | 7753.09 | 10.35 | 66.52 | 8.92 |
| P6; 0.1 | 8852.71 | 10.15 | 72.31 | 8.98 |

## 4 Conclusions

In this study, an evaluation of fibers, which are incorporated into 3D printing mortar dosages, was carried out. The fibers used were aramid, glass, carbon, cellulose, textile, zylon, and polypropylene, in five different contents: 0.05; 0.075; 0.1; 0.2; and 0.3. These contents of fiber might appear quite low; however, some authors have also determined that optimal values could be 0.1% in PVA, 0.25% in PP, or 0.5% in basalt fibers as sumarized in [13, 63].

Firstly, a certain range of values of fiber percentages added to the mortars was selected in order to avoid clogging or printing problems on the nozzle of the 3D printer based on preliminary printing trials. Then, a series of laboratory experiments were carried out on rheology, flexural, and compressive strength. Once the laboratory tests had been carried out, a life cycle and statistical analysis was performed. With all the data obtained, a multi-criteria MCMDA was carried out using the WASPAS and TOPSIS methods to select the best alternatives. In addition, these methods


**Fig. 8** Ranking (bars) and score (dots) of the alternatives with TOPSIS and WASPAS methods. **a** Scenario 1 (AHP weights); **b** Scenario 2 (equal weights)

were combined with the AHP method and equal weights of assigning weights, to give the relative importance of all the responses involved in the MCMD. The main conclusions obtained in this study are the following:

- With the incorporation of the fibers in the dosages used for 3D printing, increases in flexural strength of up to 30% were achieved, which matches previous studies. Compressive strength on fiber-reinforced mortars did not show significant changes with respect to control sample (no fibers).
- Only significant correlations between flexural strength and elastic modulus of fibers have been demonstrated through a regression model. No correlations with amount of fibers or length could be demonstrated in this study.
- As far as rheology is concerned, there is a good correspondence between the results obtained in the tests and what was shown in the laboratory when the printability tests were carried out. As the fiber content increased, the mixtures showed worse workability characteristics, to the point that with certain amounts of fibers the filaments began to break or block at the nozzle and the mortars were no longer suitable for printing. With the rheological results, as the fiber content increased, yield stress values increased significantly, as also reported in [45].

- With respect to the LCA results, no very notable differences were obtained between the different dosages analyzed. This is due to the fact that the fibers represent a small part of the dosage and are not the part that has the greatest effect on the LCA result. However, a quantification of their impact is now available.
- In relation to the AHP method of assigning weights to the different criteria, the greatest weight was given to printability (38.14%), followed by strength (27.17%), environmental impact (21.83%), and cost (12.86%). However, since the relative difference among alternatives in terms of environmental impact and strength was not that high, printability and cost were the criteria that affect more the MCDMA analysis.
- The WASPAS and TOPSIS methods, in the two scenarios, yield the following ranking with the best 3 dosages: G13;0.1 (1st position always), Cell6;0.05 (2nd position in Scenario 2; 3rd position in Scenario 1), C25;0.05 (2nd position in Scenario 1; 3rd position in Scenario 2), showing that the dosages with lower fiber contents present better results. On the other hand, zylon and aramid fibers were ranked in the last positions mainly due to their high costs.
- Mortars with textile fibers, even though their cost is null (it is a residue), were ranked in relatively bottom positions (21 in the best case: Scenario 2, "T20;0.5," WASPAS), since their increase in flexible strength was quite low and its printability was also poor.
- Control sample (no fibers) was ranked between 4 to 10 position, depending on weighting scenario and ranking method.

As an overall conclusion, it could be stated that certain low-medium cost fibers like glass, cellulose, or carbon could increase the flexural strength without compromising cost, printability, and environmental impact, by adding 0.05 to 0.1% in weight depending on the case. Besides, other highly resistant fibers such as aramid or zylon are not cost-effective solutions to increase flexural strength in 3D printing mortar. Also, the option of not using fibers should also be considered, since it was ranked in between 4 and 10th position, much better than highly resistant fibers.

**Acknowledgements** The authors would like to thank the following companies for their contributions: Cementos Portland Valderribas S.A for providing the cement, Basf Chemicals Ltd. for providing all the additives, Teijin Limited Ltd. for providing various types of fibers (aramid, carbon, and zylon), Fibratec Técnicas de la Fibra S.L for providing the glass fibers, and Textil Santanderina S.A. for providing the textile fibers.

**Author contribution** Elena Blanco-Fernandez, Daniel Castro, and Sara Alonso-Cañon contributed to the study conception and design. Material preparation and laboratory tests were mainly performed by Sara Alonso-Cañon with the help of Adrian I. Yoris-Nobile. Analysis of results and conclusions were performed by Sara Alonso-Cañon and Elena Blanco-Fernandez. Laura Castañon-Jano contributed mainly to the MCDM analysis. The first draft of the manuscript was mainly written by Sara Alonso-Cañon and all authors commented and improved previous versions of the manuscript. New versions of the manuscript during the revision process have been undertaken by Elena Blanco. All authors read and approved the final manuscript.

**Funding** Open Access funding provided thanks to the CRUE-CSIC agreement with Springer Nature. • The work has received funding from the Spanish Ministry of Science and Innovation through three grants:

• "Promotion of activity in R + D of GITECO and GCS groups of the University of Cantabria" (Ref: SSPJO1900I001723XV0)

• "Fostering the circular economy and low CO2 technologies through the additive manufacturing -3DCircle-" (Ref: PID2020-112851RA-I00).

• "Enhancing biodiversity in the Atlantic area through sustainable artificial reefs -EBASAR-" (Ref: TED2021-129532B-I00).

## Declarations

**Conflict of interest** The authors declare no competing interests.



## References

1. Arunothayan AR, Nematollahi B, Ranade R, Bong SH, Sanjayan J (2020) Development of 3D-printable ultra-high performance fiber-reinforced concrete for digital construction. Constr Build Mater 257:119546. https://doi.org/10.1016/j.conbuildmat.2020.119546
2. Pham L, Tran P, Sanjayan J (2020) Steel fibres reinforced 3D printed concrete: influence of fibre sizes on mechanical performance. Constr Build Mater 250:118785. https://doi.org/10.1016/j.conbuildmat.2020.118785
3. Korniejenko K et al (2020) Mechanical properties of short fiber-reinforced geopolymers made by casted and 3D printing methods: a comparative study. Materials 13(3):579. https://doi.org/10.3390/ma13030579
4. Hambach M, Möller H, Neumann T, Volkmer D (2016) Portland cement paste with aligned carbon fibers exhibiting exceptionally high flexural strength (> 100 MPa). Cem Concr Res 89:80–86. https://doi.org/10.1016/j.cemconres.2016.08.011
5. Panda B, Chandra Paul S, Jen Tan M (2017) Anisotropic mechanical performance of 3D printed fiber reinforced sustainable construction material. Mater Lett 209:146–149. https://doi.org/10.1016/j.matlet.2017.07.123
6. Chu SH, Li LG, Kwan AKH (2021) Development of extrudable high strength fiber reinforced concrete incorporating nano calcium

carbonate. Addit Manuf 37:101617. https://doi.org/10.1016/j.addma.2020.101617
7. Soltan DG, Li VC (2018) A self-reinforced cementitious composite for building-scale 3D printing. Cem Concr Compos 90:1–13. https://doi.org/10.1016/j.cemconcomp.2018.03.017
8. Jo JH. Jo BW, Cho W, Kim J-H (2020) Development of a 3D printer for concrete structures: laboratory testing of cementitious materials. Int J Concr Struct Mater 14(1). https://doi.org/10.1186/s40069-019-0388-2
9. Al-Qutaifi S, Nazari A, Bagheri A (2018) Mechanical properties of layered geopolymer structures applicable in concrete 3D-printing. Constr Build Mater 176:690–699. https://doi.org/10.1016/j.conbuildmat.2018.04.195
10. Nematollahi B et al (2018) Effect of polypropylene fibre addition on properties of geopolymers made by 3D printing for digital construction. Materials 11(12). https://doi.org/10.3390/ma11122352
11. Fisher AK, Bullen F, Beal D (2001) The durability of cellulose fibre reinforced concrete pipes in sewage applications. Cem Concr Res 31(4):543–553. https://doi.org/10.1016/S0008-8846(00)00451-8
12. MacVicar R, Matuana LM, Balatinecz JJ (1999) Aging mechanisms in cellulose fiber reinforced cement composites. Cem Concr Compos 21(3):189–196. https://doi.org/10.1016/S0958-9465(98)00050-X
13. Alonso-Canon S, Blanco-Fernandez E, Castro-Fresno D, Yoris-Nobile AI, Castañon-Jano L (2022) Reinforcements in 3D printing concrete structures. Arch Civ Mech Eng 23(1):25
14. Inozemtcev A, Duong TQ (2019) Technical and economic efficiency of materials using 3D-printing in construction on the example of high-strength lightweight fiber-reinforced concrete. In E3S Web of Conferences. https://doi.org/10.1051/e3sconf/20199702010
15. Kreiger EL, Kreiger MA, Case MP (2019) Development of the construction processes for reinforced additively constructed concrete. Addit Manuf 28:39–49. https://doi.org/10.1016/j.addma.2019.02.015
16. García de Soto B et al (2018) Productivity of digital fabrication in construction: cost and time analysis of a robotically built wall. Autom Constr 92:297–311. https://doi.org/10.1016/j.autcon.2018.04.004
17. Nerella VN, Krause M, Mechtcherine V (2020) Direct printing test for buildability of 3D-printable concrete considering economic viability. Autom Constr 109. https://doi.org/10.1016/j.autcon.2019.102986
18. Otto J, Kortmann J, Krause M (2020) Cost calculation of concrete 3D printing [Wirtschaftliche Perspektiven von Beton-3D-Druckverfahren]. Beton- und Stahlbetonbau 115(8):586–597. https://doi.org/10.1002/best.201900087
19. Han Y, Yang Z, Ding T, Xiao J (2021) Environmental assessment of large-scale 3D printing in construction: a comparative study between cob and concrete. J Clean Prod 278. https://doi.org/10.1016/j.jclepro.2020.123884
20. Abdalla H, Fattah KP, Abdallah M, Tamimi AK (2021) Environmental footprint and economics of a full-scale 3d-printed house. Sustainability (Switzerland) 13(21). https://doi.org/10.3390/su132111978
21. Weng Y et al (2020) Comparative economic, environmental and productivity assessment of a concrete bathroom unit fabricated through 3D printing and a precast approach. J Clean Prod 261. https://doi.org/10.1016/j.jclepro.2020.121245
22. Yoris-Nobile AI et al (2022) Life cycle assessment (LCA) and multi-criteria decision-making (MCDM) analysis to determine the performance of 3D printed cement mortars and geopolymers. J Sustain Cem Based Mater. https://doi.org/10.1080/21650373.2022.2099479
23. Pons-Valladares O, del Mar Casanovas-Rubio M, Armengou J, de la Fuente A (2023) Approach for sustainability assessment for footbridge construction technologies: application to the first world D-shape 3D-printed fiber-reinforced mortar footbridge in Madrid. J Clean Prod 394. https://doi.org/10.1016/j.jclepro.2023.136369
24. Alhumayani H, Gomaa M, Soebarto V, Jabi W (2020) Environmental assessment of large-scale 3D printing in construction: a comparative study between cob and concrete. J Clean Prod 270. https://doi.org/10.1016/j.jclepro.2020.122463
25. Mohammad M, Masad E, Al-Ghamdi SG (2020) 3d concrete printing sustainability: a comparative life cycle assessment of four construction method scenarios. Buildings 10(12):1–20. https://doi.org/10.3390/buildings10120245
26. Jayathilakage R, Rajeev P, Sanjayan J (2022) Rheometry for concrete 3D printing: a review and an experimental comparison. Buildings 12(8). https://doi.org/10.3390/buildings12081190
27. Chen M et al (2020) Rheological parameters and building time of 3D printing sulphoaluminate cement paste modified by retarder and diatomite. Constr Build Mater 234. https://doi.org/10.1016/j.conbuildmat.2019.117391
28. Kolawole JT, Combrinck R, Boshoff WP (2019) Measuring the thixotropy of conventional concrete: the influence of viscosity modifying agent, superplasticiser and water. Constr Build Mater 225:853–867. https://doi.org/10.1016/j.conbuildmat.2019.07.240
29. Banfill PFG (2011) Additivity effects in the rheology of fresh concrete containing water-reducing admixtures. Constr Build Mater 25(6):2955–2960. https://doi.org/10.1016/j.conbuildmat.2010.12.001
30. Chen M et al (2020) Rheological parameters, thixotropy and creep of 3D-printed calcium sulfoaluminate cement composites modified by bentonite. Compos B Eng 186. https://doi.org/10.1016/j.compositesb.2020.107821
31. Roussel N (2018) Rheological requirements for printable concretes. Cem Concr Res 112:76–85. https://doi.org/10.1016/j.cemconres.2018.04.005
32. Ramezanianpour AA, Esmaeili M, Ghahari SA, Najafi MH (2013) Laboratory study on the effect of polypropylene fiber on durability, and physical and mechanical characteristic of concrete for application in sleepers. Constr Build Mater 44:411–418. https://doi.org/10.1016/j.conbuildmat.2013.02.076
33. Zhang D, Yu J, Wu H, Jaworska B, Ellis BR, Li VC (2020) Discontinuous micro-fibers as intrinsic reinforcement for ductile engineered cementitious composites (ECC). Compos B Eng 184. https://doi.org/10.1016/j.compositesb.2020.107741
34. Soualhi H, Kadri E-H, Ngo T-T, Bouvet A, Cussigh F, Tahar Z-E-A (2017) Design of portable rheometer with new vane geometry to estimate concrete rheological parameters. J Civ Eng Manag 23(3):347–355. https://doi.org/10.3846/13923730.2015.1128481
35. Laskar AI, Bhattacharjee R (2011) Torque-speed relationship in a concrete rheometer with vane geometry. Constr Build Mater 25(8):3443–3449. https://doi.org/10.1016/j.conbuildmat.2011.03.035
36. Soualhi H, Kadri EH, Ngo TT, Bouvet A, Cussigh F, Kenai S (2014) A vane rheometer for fresh mortar: development and validation. Appl Rheol 24(2). https://doi.org/10.3933/ApplRheol-24-22594
37. Banfill PFG (2003) The rheology of fresh cement and concrete – a review. In Proc 11th International Cement Chemistry Congress, Durban, May 2003
38. Lanos C, Estellé P (2009) Vers une réelle rhéométrie adaptée aux bétons frais. Revue européenne de génie civil 13(4):457–471. https://doi.org/10.3166/ejece.13.257-471
39. Estellé P, Lanos C, Perrot A (2008) Processing the Couette viscometry data using a Bingham approximation in shear rate

calculation. J Nonnewton Fluid Mech 154(1):31–38. https://doi.org/10.1016/j.jnnfm.2008.01.006
40. Wille K, El-Tawil S, Naaman AE (2014) Properties of strain hardening ultra high performance fiber reinforced concrete (UHP-FRC) under direct tensile loading. Cem Concr Compos 48:53–66. https://doi.org/10.1016/j.cemconcomp.2013.12.015
41. Japanese Society of Civil Engineer (1984) JSCE-SF4. Method of test for flexural strength and flexural toughness of steel fiber reinfocerd concrete. [Online]. Available: http://library.jsce.or.jp/Image_DB/spec/con_lib/no03/CLIno03_0058.pdf.Accessed 31 Aug. 2023
42. ASTM, ASTM C1018–97 (1997) Standard test method for flexural toughness and first-crack strength of fiber-reinforced concrete (Using beam with third-point loading) (Withdrawn 2006). https://www.astm.org/c1018-97.html
43. CEN- European Committee for Standardization (2016) EN 196–1:2016. Methods of testing cement. Part 1: Determination of strength. https://standards.cencenelec.eu/
44. ACI Committee 544 (2002) Report on fiber reinforced concrete. https://www.concrete.org/Portals/0/Files/PDF/Previews/544.4R-18_preview.pdf
45. Khan MI, Abbas YM, Fares G (2017) Review of high and ultra-high performance cementitious composites incorporating various combinations of fibers and ultrafines. J King Saud Univ-Eng Sci 29(4):339–347. https://doi.org/10.1016/j.jksues.2017.03.006
46. Wang C, Chen B, Vo TL, Rezania M (2023) Mechanical anisotropy, rheology and carbon footprint of 3D printable concrete: a review. J Building Eng 76. https://doi.org/10.1016/j.jobe.2023.107309
47. Yoris-Nobile AI (2023) Manufacture of artificial reefs by 3d printing using sustainable mortars. PhD Thesis., Universidad de Cantabria, Santander, 2023. [Online]. Available: https://hdl.handle.net/10902/28426. Accessed 01 Sep. 2023
48. International Organization for Standardization (2006) ISO 14040: Environmental management - life cycle assessment - principles and framework, 2nd edn. https://www.iso.org/standard/37456.html
49. International Organization for Standardization (2006) ISO 14044: Environmental management - life cycle assessment - requirements and guidelines, 1st edn. https://www.iso.org/standard/38498.html
50. Wernet G, Bauer C, Steubing B, Reinhard J, Moreno-Ruiz E, Weidema B (2016) The ecoinvent database version 3 (part I): overview and methodology. Int J Life Cycle Assess 21(9):1218–1230. https://doi.org/10.1007/s11367-016-1087-8
51. Stengel T, Reger J, Heinz D (2009) Life cycle assessment of geopolymer concrete – what is the environmental benefit? In Concrete Solutions 09. 24th Biennial Conf Australian Concrete Institute, 2009. [Online]. Available: https://www.researchgate.net/profile/Thorsten-Stengel/publication/373107380_Life_Cycle_Assessment_of_Geopolymer_Concrete_-_What_is_the_Environmental_Benefit/links/64d9e461ad846e288290459e/Life-Cycle-Assessment-of-Geopolymer-Concrete-What-is-the-Environmental-Benefit.pdf. Accessed 09 May 2024
52. Turner LK, Collins FG (2013) Carbon dioxide equivalent (CO<inf>2</inf>-e) emissions: a comparison between geopolymer and OPC cement concrete. Constr Build Mater 43:125–130. https://doi.org/10.1016/j.conbuildmat.2013.01.023
53. Cao K et al (2012) Synthesis and characterization of poly(p -phenylene benzobisoxazole)/poly(pyridobisimidazole) block copolymers. J Macromol Sci Part A Pure Appl Chem 49(6):508–517. https://doi.org/10.1080/10601325.2012.676924
54. Crenna E, Secchi M, Benini L, Sala S (2019) Global environmental impacts: data sources and methodological choices for calculating normalization factors for LCA. Int J Life Cycle Assess 24(10):1851–1877. https://doi.org/10.1007/s11367-019-01604-y
55. Sala S, Cerutti A, Pant R (2017) Development of a weighting approach for the environmental footprint. EUR 28562 EN. https://op.europa.eu/en/publication-detail/-/publication/6c24e876-4833-11e8-be1d-01aa75ed71a1
56. Zavadskas EK, Turskis Z, Antucheviciene J, Zakarevicius A (2012) Optimization of weighted aggregated sum product assessment. Elektronika ir Elektrotechnika 122(6):3–6. https://doi.org/10.5755/j01.eee.122.6.1810
57. Mardani A et al (2017) A systematic review and meta-Analysis of SWARA and WASPAS methods: theory and applications with recent fuzzy developments. Appl Soft Comput 57:265–292. https://doi.org/10.1016/j.asoc.2017.03.045
58. Hwang C-L, Yoon K (1981) Multiple attribute decision making. Methods and applications. A state-of-the-art survey. Springer Link, Heidelberg. https://doi.org/10.1007/978-3-642-48318-9
59. Salih MM, Zaidan BB, Zaidan AA, Ahmed MA (2019) Survey on fuzzy TOPSIS state-of-the-art between 2007 and 2017. Comput Oper Res 104:207–227. https://doi.org/10.1016/j.cor.2018.12.019
60. Saaty TL (1977) A scaling method for priorities in hierarchical structures. J Math Psychol 15(3):234–281. https://doi.org/10.1016/0022-2496(77)90033-5
61. Hambach M, Volkmer D (2017) Properties of 3D-printed fiber-reinforced Portland cement paste. Cem Concr Compos 79:62–70. https://doi.org/10.1016/j.cemconcomp.2017.02.001
62. Peyvandi A, Soroushian P, Jahangirnejad S (2013) Enhancement of the structural efficiency and performance of concrete pipes through fiber reinforcement. Constr Build Mater 45:36–44. https://doi.org/10.1016/j.conbuildmat.2013.03.084
63. Liu X, Li J, Li Q, Hou G (2023) Mechanical performance optimization in spray-based three-dimensional-printed mortar using carbon fiber. J Mater Civil Eng 35(2). https://doi.org/10.1061/(ASCE)MT.1943-5533.0004587